Electronic Supplementary Information (ESI)

Nano-Bio Interactions of Gum Arabic-Stabilized Lanthanide-based Upconverting Nanoparticles: In Vitro and In Vivo Study

Hana Mirmajidi,[a] Hyojin Lee,[b] Niepukolie Nipu,[b] Jith Thomas,[c] Zuzana Gajdosechova,[d] David Kennedy,[d] Jan A. Mennigen,*[b] and Eva Hemmer*[a]

[a] Department of Chemistry and Biomolecular Sciences, University of Ottawa, 10 Marie-Curie Private, Ottawa (ON) K1N 6N5, Canada.

[b] Department of Biology, University of Ottawa, 20 Marie-Curie Private, Ottawa (ON) K1N 6N5, Canada.

[c] Bureau of Chemical Safety, Food and Nutrition Directorate, Health Products and Food Branch, Health Canada, 251 Sir Frederick Banting Driveway, Tunney's Pasture, Ottawa (ON) K1A 0K9, Canada.

[d] Metrology, National Research Council Canada, 1200 Montreal Road, Ottawa (ON) K1A 0R6, Canada.

* Corresponding Authors E-mail:
ehemmer@uottawa.ca
jan.mennigen@uottawa.ca

Table of Contents

1. Additional Experimental Details

Ligand-free Ln-NPs (Ln-NPs-LF). Ln-NPs-LF were obtained through acidic treatment of the OA-capped Ln-NPs following a previously established protocol.[1] In brief, approximately 150 mg of OA-capped Ln-NPs were dispersed in 15 mL of hexane and transferred to a 125 mL Erlenmeyer flask. To this suspension, 15 mL of an aqueous solution of HCl (pH = 1.5) was added, resulting in a 1:1 (v:v) ratio between the organic and aqueous phase and a 5 mg/mL NP concentration. The mixture was vigorously stirred at room temperature overnight. Subsequently, the bi-phasic system (acidic aqueous phase and organic hexane phase) was separated using a separation funnel. The organic phase was discarded, while the aqueous phase was transferred to a centrifuge tube, diluted with a 1:3 ratio of a water-to-acetone mixture, and centrifuged at 9000 rpm for 20 min. This washing procedure was repeated twice after which the Ln-NPs-LF were stored in 5 mL of water for posterior characterizations. The Ln-NPs-LF were used as starting material for the synthesis of Gum Arabic-capped Ln-NPs (Ln-NPs-GA) and as one of the control samples for comparison with Ln-NPs-GA.

Polyacrylic acid-capped Ln-NPs (Ln-NPs-PAA). Ln-NPs capped with polyacrylic acid (PAA) as control sample were obtained via a ligand exchange procedure, starting from as-synthesized Ln-NPs-OA.[2] Briefly, 100 mg of OA-capped Ln-NPs were dispersed in 5 mL of chloroform, $CHCl_3$, in a 25 mL round bottom flask and mixed with 120 mg of PAA previously dissolved in 10 mL of ethanol. The mixture was left under vigorous magnetic stirring at 35 °C for 48 h. Subsequently, the Ln-NPs-PAA were precipitated by the addition of acetone (8:1 ratio of acetone-to-Ln-NP suspension), followed by centrifugation at RCF = 8346 g for 10 min. The recovered pellet was dispersed in water and washed with acetone twice (5:1 ratio of acetone-to-water). The final Ln-NPs-PAA were dispersed in 5 mL of water for further use.

2. Additional Structural Analysis by TEM, XRD, FT-IR, and TGA

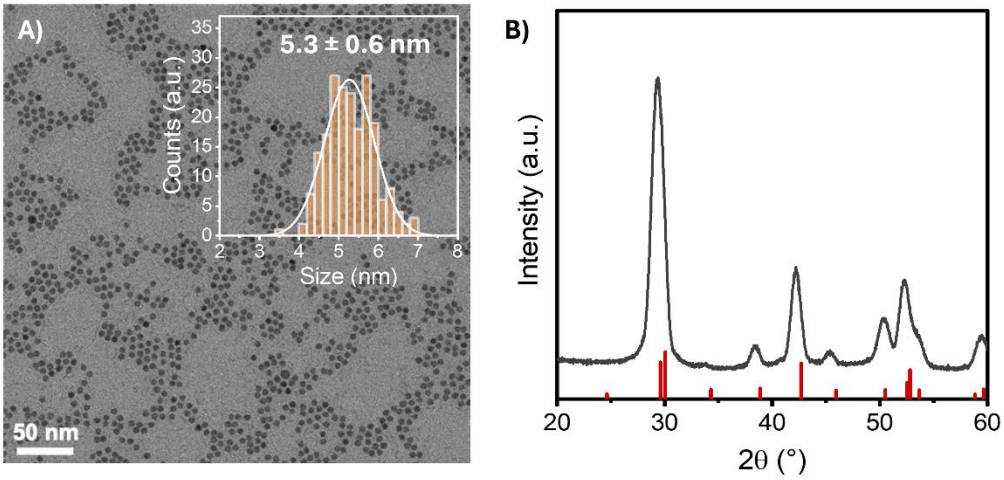

Figure S1. (A) Transmission electron microscopy (TEM) image of the oleate-capped core $NaGdF_4$:Er^{3+}/Yb^{3+} nanoparticles. Their size distribution and average size ± standard deviation is given in the inset. (B) XRD pattern of hexagonal (β-phase) core/shell Ln-NPs-OA. Reference pattern: β-$NaGdF_4$ (PDF card no. 01-080- 8787).

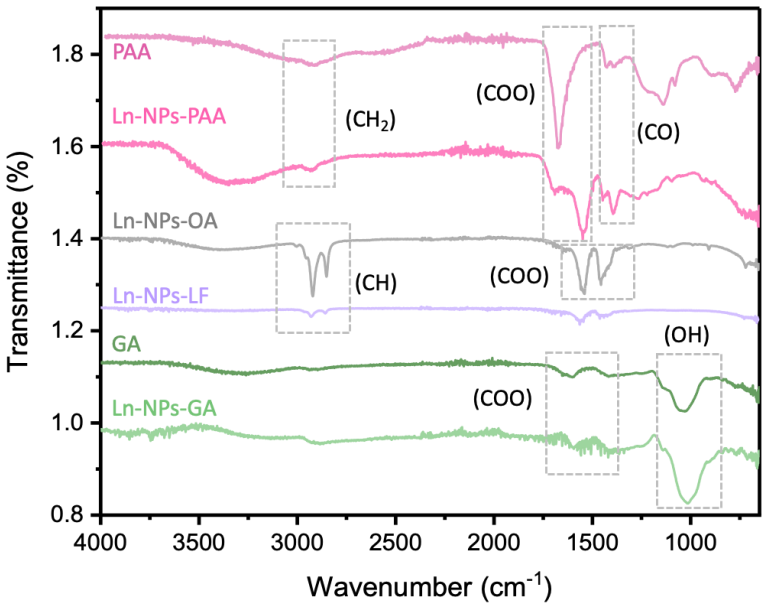

Figure S2. FT-IR spectra of Ln-NPs-GA (green line), Ln-NPs-LF (purple line), Ln-NPs-OA (grey line), and Ln-NPs-PAA (pink line) as well as pure PAA (rose line) and GA (dark green line) as references.

FT-IR spectroscopy (Figure S2) of oleate-capped Ln-NPs (Ln-NPs-OA) unveiled two peaks at 1523 and 1436 cm^{-1} that are associated with the asymmetric and symmetric stretching vibrations of the carboxylic group (-COO-), respectively.[3] In addition, two peaks at 2829 and 2902 cm^{-1} were assigned to the asymmetric and symmetric stretching vibrations, respectively, of methylene groups, which exists in the long alkyl chain of the oleic acid molecule. The disappearance of these characteristic peaks confirmed the removal of the oleate ligand from the Ln-

NPs in Ln-NPs-LF. Upon capping with GA (Ln-NPs-GA), a band at ca. 1000 cm^{-1} arose, which can be ascribed to OH^- (hydroxyl) groups, while a characteristic band for -COOH (carboxylic acid) was observed at 1600 cm^{1}.[4] These features are in good agreement with those observed in the FT-IR spectrum recorded on pure GA, providing strong evidence for the presence of GA on the surface of the Ln-NPs. Likewise, FT-IR spectra recorded on PAA and Ln-NPs-PAA showed characteristic peaks for CH_2 (methylene) groups at around 2800 cm^{-1}, COO (carboxylate) groups at around 1800 cm^{-1}, and CO (carbonyl) groups at around 1400 cm^{-1},[5] confirming the presence of PAA at the Ln-NP surface.

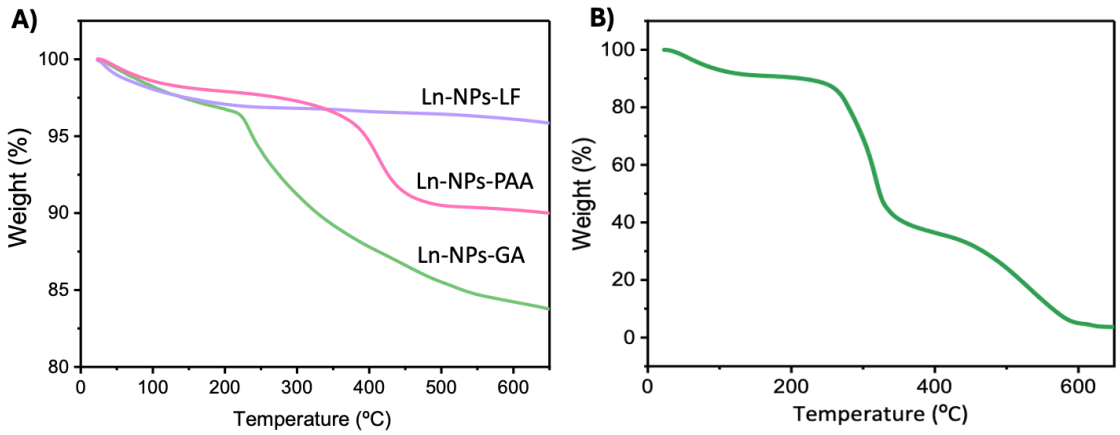

Figure S3. TGA profiles of (A) Ln-NPs-LF, Ln-NPs-PAA, and Ln-NPs-GA. (B) TGA profile of pure GA as a reference.

TG analysis was performed to provided further evidence for the presence of GA at the surface of the Ln-NPs (Figure S3). Irrespective of the surface chemistry, all samples, Ln-NPs-GA, Ln-NPs-PAA, and Ln-NPs-LF, exhibited an initial mass loss of less than 5% at ca. 100 °C, which can be ascribed to residual water (Figure S3A). As expected, Ln-NPs-LF (purple line) did not experience any further mass loss upon further temperature treatment. In contrast, Ln-NPs-PAA (pink line) showed a weight loss of ca. 8%, which was completed at ca. 500 °C, indicating the loss of PAA groups. The most significant mass loss of ca. 14% was observed for Ln-NPs-GA (green line). Moreover, the recorded TGA profile indicated a two-step mass loss. The fist mass loss took place between 200 and 400 °C, followed by a second mass loss at temperatures above 400 °C. This two-step mass loss is in good agreement with the TGA profile obtained for pure GA (Figure S3B), hence, can be ascribed to the decomposition of GA attached to the surface of the Ln-NPs.

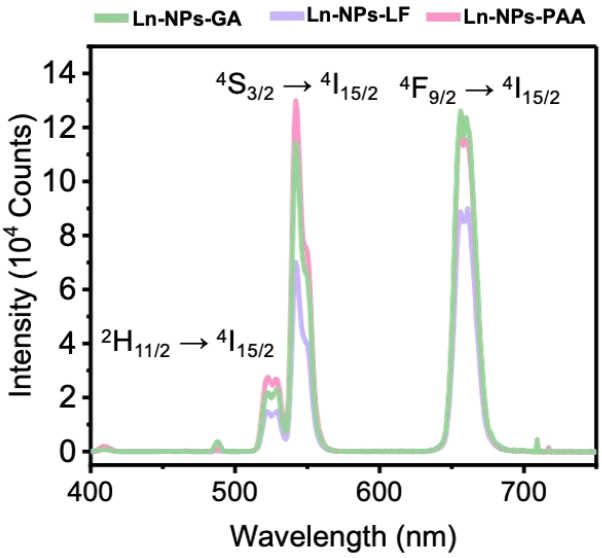

Figure S4. Upconversion emission spectra of Ln-NPs-GA, Ln-NPs-PAA, and Ln-NPs-LF dispersed in water under 980 nm excitation (laser power density: 6.7 W/cm^2, particle concentration: 4 mg/mL).

3. Colloidal and Optical Stability of Ln-NPs-LF and Ln-NPs-PAA

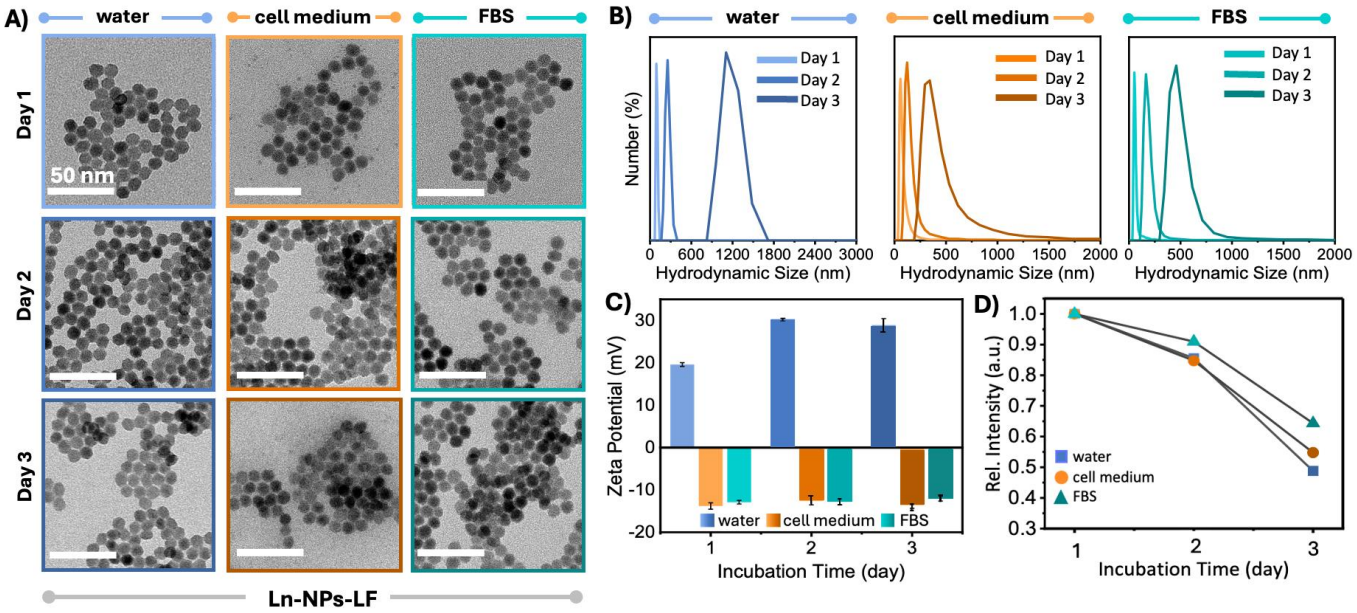

Figure S5. Analysis of the colloidal and optical stability of Ln-NPs-LF dispersed in water (blue), cell culture medium (orange), and FBS (teal). (A) TEM images of Ln-NPs-LF recorded on freshly dispersed Ln-NPs-LF (day 1), after 24 h (day 2), and 48 h (day 3); scale bars: 50 nm. (B) DLS curves of Ln-NPs-LF dispersed in water, cell culture medium, and FBS, respectively, recorded at days 1, 2, and 3 of storage in the respective media. DLS data revealed a change in hydrodynamic diameters of Ln-NPs-LF from ca. 90 to 1100 nm in water (PDI: 0.43), ca. 60 to 340 nm in cell culture medium (PDI: 0.55), and ca. 50 to 460 nm in FBS (PDI: 0.98). (C) Zeta potential of Ln-NPs-LF dispersed in water, cell culture medium, and FBS, respectively, recorded at days 1, 2, and 3 of storage in the respective media. All zeta potential data are presented as mean value ± standard deviation based on triplicate measurements taken for each sample in each of the three solvents at each time point. Error bars, representing the standard deviation, derived from these triplicate measurements. (D) Change in the overall upconversion emission intensity of the Ln-NPs-LF as a function of storage in water, cell culture medium, and FBS. Data represent the integrated intensity in the 510 to 695 nm spectral range (spectra are shown in Figure S7).

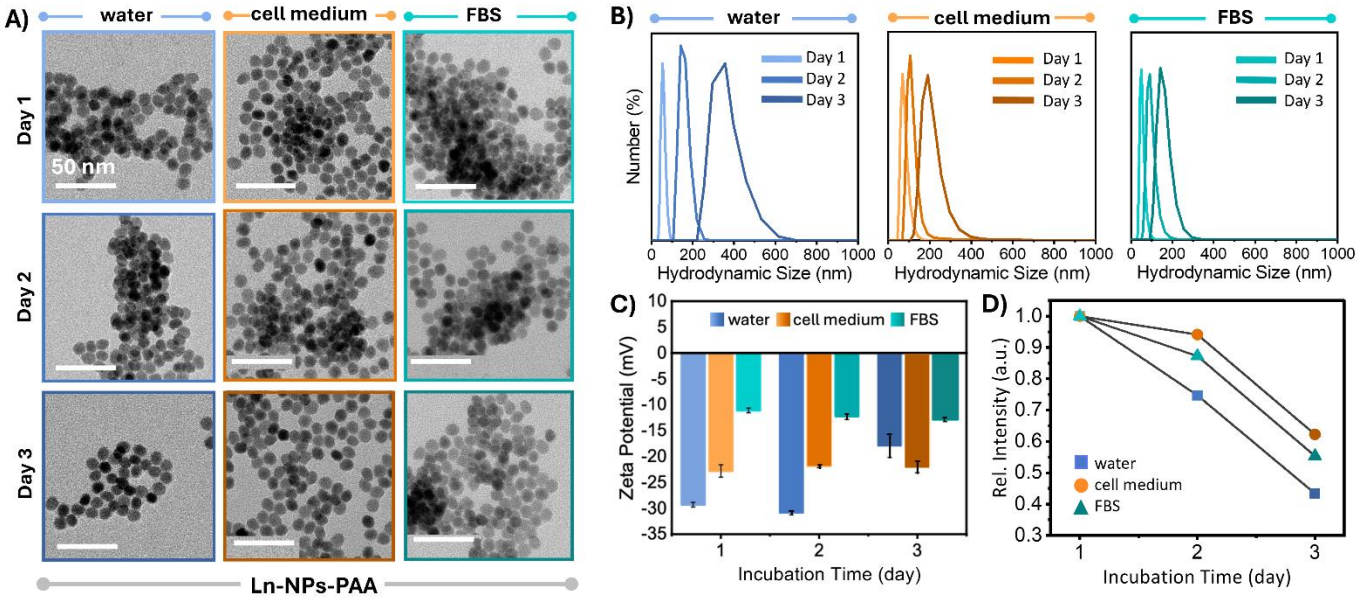

Figure S6. Analysis of the colloidal and optical stability of Ln-NPs-PAA dispersed in water (blue), cell culture medium (orange), and FBS (teal). (A) TEM images of Ln-NPs-PAA recorded on freshly prepared Ln-NPs-PAA (day 1) as well as after incubation for 24 h (day 2) and 48 h (day 3); scale bars: 50 nm. (B) DLS curves of Ln-NPs-LF dispersed in water, cell culture medium, and FBS, respectively, recorded at days 1, 2, and 3 of storage in the respective media. DLS data revealed an increase in hydrodynamic diameters of Ln-NPs-PAA from ca. 50 to 360 nm in water (PDI: 0.64), ca. 70 to 190 nm in cell culture medium (PDI: 0.49), and ca. 50 to 140 nm in FBS (PDI: 0.58). (C) Zeta potential of Ln-NPs-PAA dispersed in water, cell culture medium, and FBS, respectively, recorded at days 1, 2, and 3 of storage in the respective media. All zeta potential data are presented as mean value ± standard deviation based on triplicate measurements taken for each sample in each of the three solvents at each time point. Error bars, representing the standard deviation, derived from these triplicate measurements. (D) Change in the overall upconversion emission intensity of the Ln-NPs-PAA as a function of storage in water, cell culture medium, and FBS. Data represent the integrated intensity in the 510 to 695 nm spectral range (spectra are shown in Figure S7).

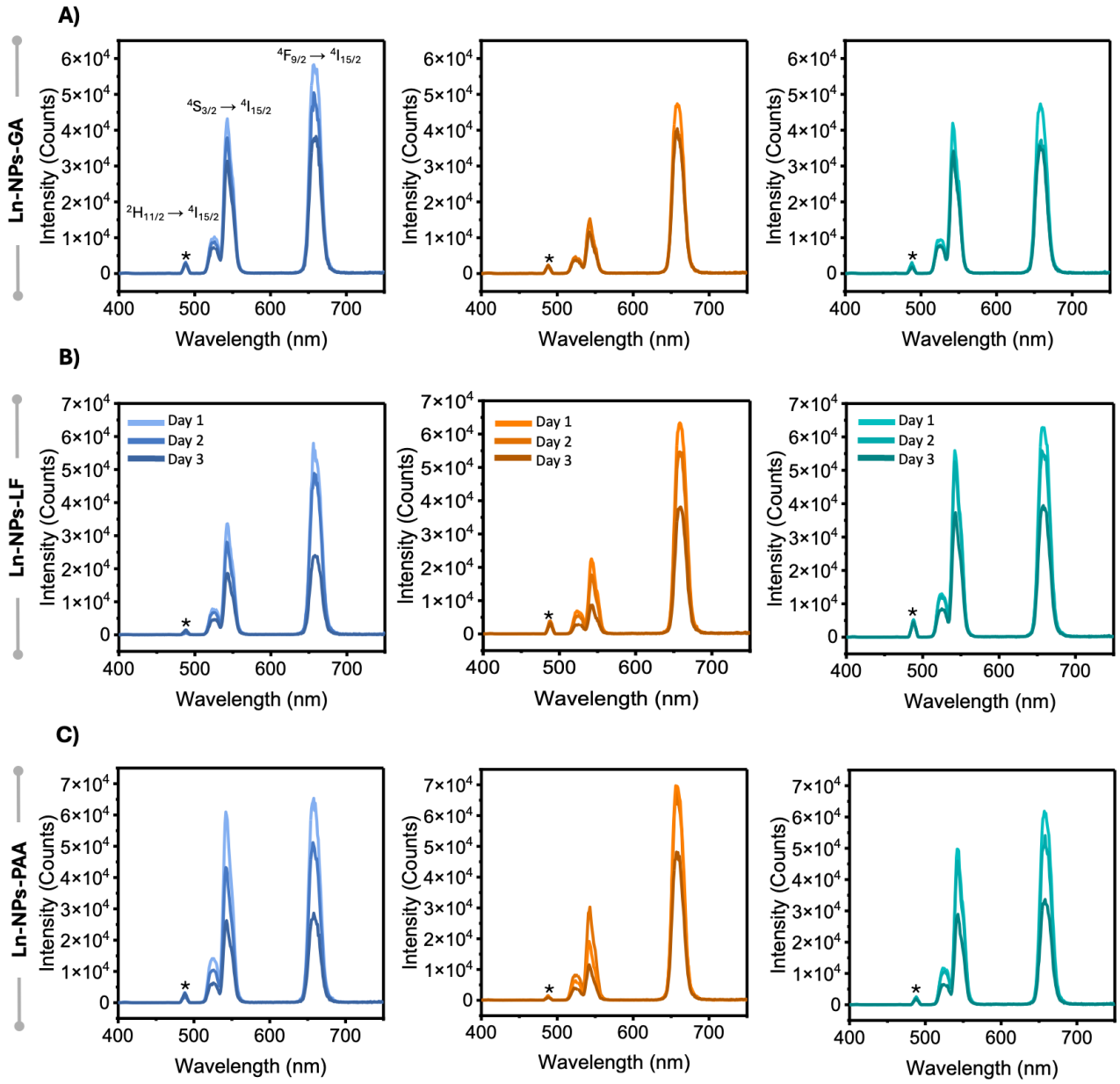

Figure S7. Time-dependent upconversion emission intensity of (A) Ln-NPs-GA, (B) Ln-NPs-LF, and (C) Ln-NPs-PAA dispersed in water (blue), cell culture medium (orange), and FBS (teal). Ln-NP concentrations in the respective aqueous media as determined by ICP: Ln-NPs-GA: 0.4 mg/mL, Ln-NPs-LF: 0.8 mg/mL, and Ln-NPs-PAA: 0.8 mg/mL. The weak peak at 490 nm – marked with * – stems from the 980 nm excitation laser. Laser power density: 13.33 W/cm^2. Noteworthy, emission intensities in the same order of magnitude were obtained for all Ln-NPs, despite the significantly lower concentration of Ln-NPs-GA. This suggests that GA provided good protection from solvent quenching effects, allowing for strong upconversion emission.

4. NIR Emission Spectra

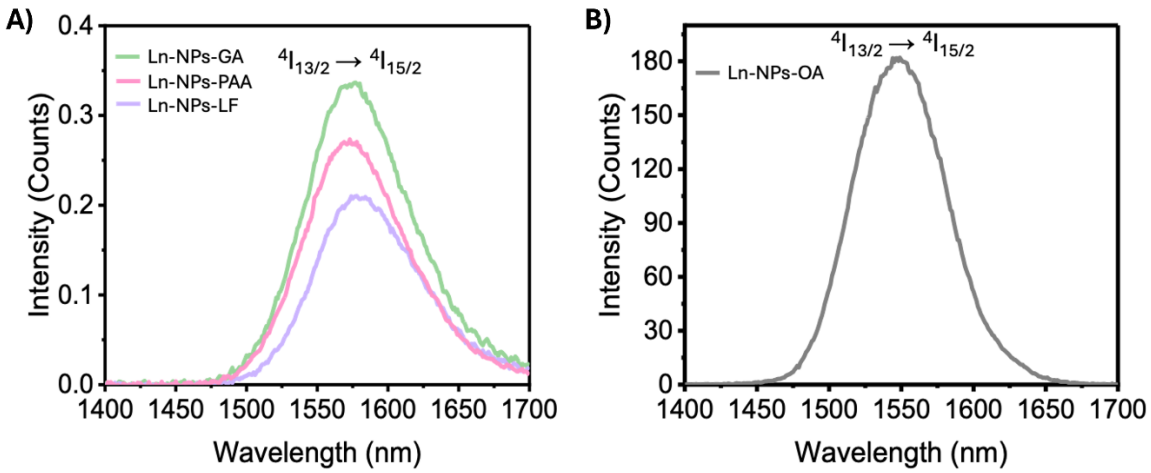

Figure S8. NIR emission spectra of (A) Ln-NPs-GA, Ln-NPs-LF, and Ln-NPs-PAA (dispersed in water) and (B) OA-capped Ln-NPs (dispersed in toluene). λ_{ex} = 980 nm. Laser power density: 38.7 W/cm². Ln-NP concentration: ca. 4 mg/mL.

Similar to trends observed for the upconversion emission, the surface capping played a crucial role in maintaining the stability of Ln-NPs under physiological conditions. Gum Arabic, being an excellent stabilizing agent, efficiently prevented agglomeration, thereby preserving the optical properties of the nanoparticles more effectively than PAA or in the absence of any capping agent (Ln-NPs-LF) (Figure S8A). Moreover, the sterically bulky GA molecules may offer better passivation from interaction of the optically active Ln^{3+} with water molecules, reducing non-radiative losses in aqueous environments. As expected, the NIR emission of Ln-NPs-OA was significantly higher in toluene than in water due to quenching by water molecules (Figure S8B). Still, the observed NIR emission in water renders Ln-NPs-GA promising probes operating in the NIR-III transparency window.

5. Cellular and Zebrafish Uptake

5.1 Cellular uptake: number of Ln-NPs per cell

To estimate the degree of Ln-NP uptake, the number of Ln-NPs per cell was calculated based on ICP-MS and TEM analyses. ICP-MS was used to quantify the total amount of gadolinium (Gd^{3+}) in one million cells. TEM was employed to determine the average size and volume of the spherical Ln-NPs. Moreover, crystallographic data for β-$NaGdF_4$ were used as reported in the literature.

$NaGdF_4$ NPs synthesized in this study crystallized in the hexagonal crystalline phase. Hence, the volume of one unit cell of β-$NaGdF_4$ can be determined following Equation S1:[6]

$$V_{hexagonal} = \frac{2\sqrt{3}}{4}\, a_h^2\, c_h \qquad \text{Eq. S1}$$

With a_h and c_h being the lattice parameters describing the hexagonal unit cells (a_h = 6.0304 Å, c_h = 3.6111 Å; PDF reference card: 01-080-8787).

A spherical morphology for the Ln-NPs was assumed based on TEM analysis, which allowed to calculate the volume of one Ln-NP using Equation S2:

$$V_{NP} = \frac{4}{3}\pi \left(\frac{d}{2}\right)^3 \qquad \text{Eq. S2}$$

With *d* being the diameter of the Ln-NPs as determined by TEM.

Using Equations S1 and S2, the number of Gd^{3+} ions per Ln-NP was obtained by Equation S3:

$$N_{Gd/NP} = \frac{V_{NP}}{V_{hexagonal}} \times Z \times N_{Gd/formula} \qquad \text{Eq. S3}$$

With $N_{Gd/formula}$ being the number of Gd^{3+} ions per stoichiometric formula, and Z being the number of formulas per unit cell (Z = 1 for the hexagonal $NaGdF_4$ lattice).

To determine the total number of Ln-NPs in the sample (i.e., cells incubated with Ln-NPs), first, the total molar amount of Gd^{3+}, C_{Gd}, was calculated based on the mass concentration, C_{mass}, of Gd^{3+} as determined by ICP-MS (Equation S4):

$$C_{Gd}(mmol/L) = \frac{C_{mass}}{M_{Gd}} \qquad \text{Eq. S4}$$

With M_{Gd} being the molar mass of Gd^{3+}, i.e., 157.25 g/mol.

Using the total molar amount of Gd^{3+} (Equation S4), the total number of Gd^{3+} ions in the sample, N_{Gd}, was determined following Equation S5:

$$N_{Gd} = C_{Gd} \times N_A \qquad \text{Eq. S5}$$

With $N_A = 6.022 \times 10^{23}$ mol^{-1}.

The total number of Ln-NPs in the sample was then determined by dividing the total number of Gd^{3+} ions, N_{Gd}, (Equation S5) by the number of Gd^{3+} ions per particle, $N_{Gd/NP}$ (Equation S3):

$$N_{NP} = \frac{N_{Gd}}{N_{Gd/NP}} \qquad \text{Eq. S6}$$

To determine the average number of Ln-NPs per cell, the total number of Ln-NPs obtained by Equation S6 was divided by one million, i.e., the number of cells subjected to ICP analysis (Equation S7):

$$NPs\ per\ cell\ = \frac{N_{NP}}{10^6} \qquad \text{Eq. S7}$$

The results obtained as a function of Ln-NP surface chemistry and cell line are summarized in Table S1.

Table S1. Number of Ln-NPs per cell (results were rounded to the nearest whole number).

Ln-NPs	Number of NPs per Cell		
	HepG2	U-87 MG	J774A.1
Ln-NPs-GA	135,847	815,084	3,849,008
Ln-NPs-LF	2,626,382	2,852,794	12,407,391
Ln-NPs-PAA	5,615,023	1,2497,955	32,648,645

5.2 Uptake of Ln-NPs by zebrafish

Table S2. The average amount of Ln^{3+} ions [ppm] as determined by ICP-OES analysis and the corresponding average uptake [%] of Ln-NPs by zebrafish 1 and 5 dpf. Added [Ln^{3+}]: 125 ppm. The values are average amounts and ± represent the standard deviation based on three measurements.

Time Point	Ln-NPs	Ln^{3+} in Zebrafish [ppm]	Uptake [%]
1 dpf	Ln-NPs-GA	0.28±0.02	0.2
	Ln-NPs-LF	1.76±0.22	1.4
	Ln-NPs-PAA	0.43±0.01	0.3
5 dpf	Ln-NPs-GA	0.48±0.03	0.4
	Ln-NPs-LF	1.39±0.03	1.1
	Ln-NPs-PAA	100% mortality	100% mortality

6. Hyperspectral Imaging of Zebrafish

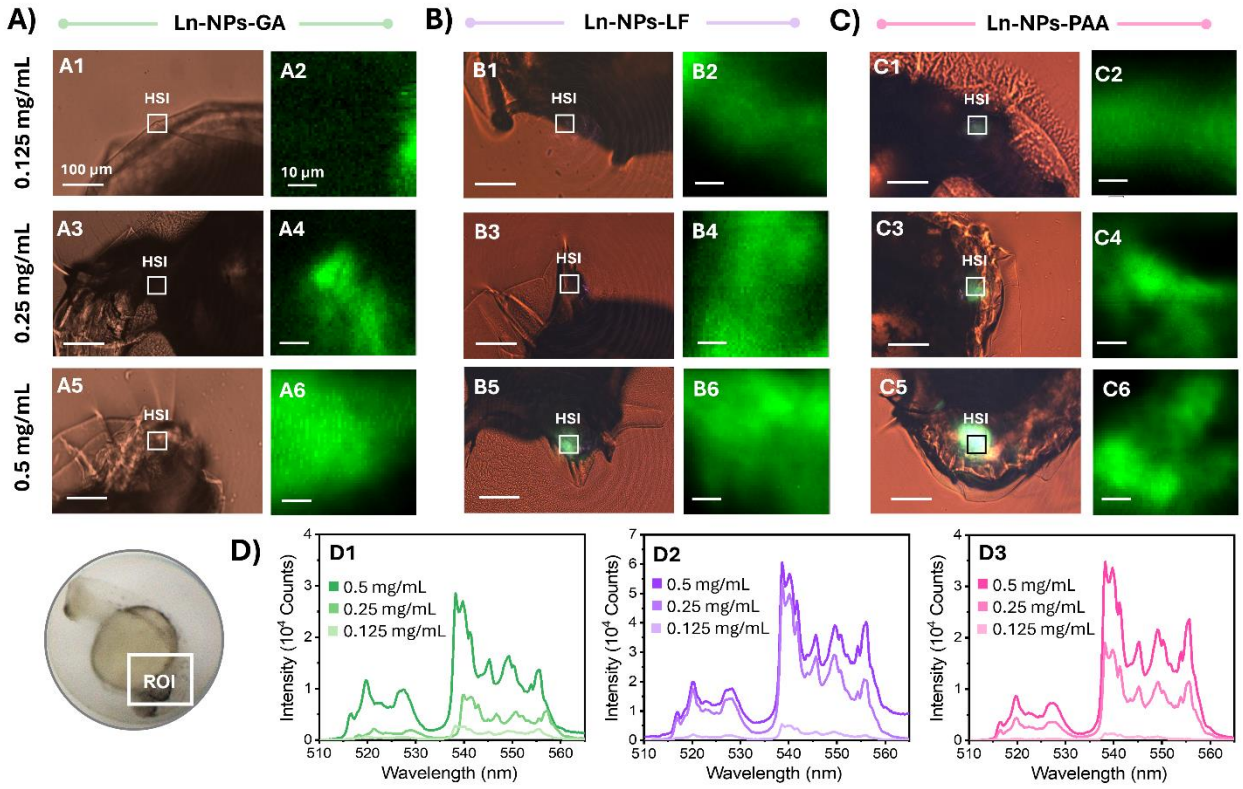

Figure S9. Bright field optical microscopy images of zebrafish 1 dpf exposed to 0.125, 0.25, and 0.5 mg/mL of (A1/3/5) Ln-NPs-GA, (B1/3/5) Ln-NPs-LF, and (C1/3/5) Ln-NPs-PAA, respectively. The images show comparable parts of zebrafish embryos as highlighted by the ROI-marked region in the light microscope image shown in the bottom left. Images were taken using a 20x objective. Scale bars are 100 µm. Hyperspectral images taken on the regions highlighted by the white rectangles labelled "HSI" of zebrafish exposed to (A2/4/6) Ln-NPs-GA, (B2/4/6) Ln-NPs-LF, and (C2/4/6) Ln-NPs-PAA. Scale bars are 5 µm. (D1–3) Spectral profiles of the areas mapped by HSI, showing the green emission spectral signature (510–568 nm) specific to the Er^{3+} dopant ions.

7. Zebrafish Deformity

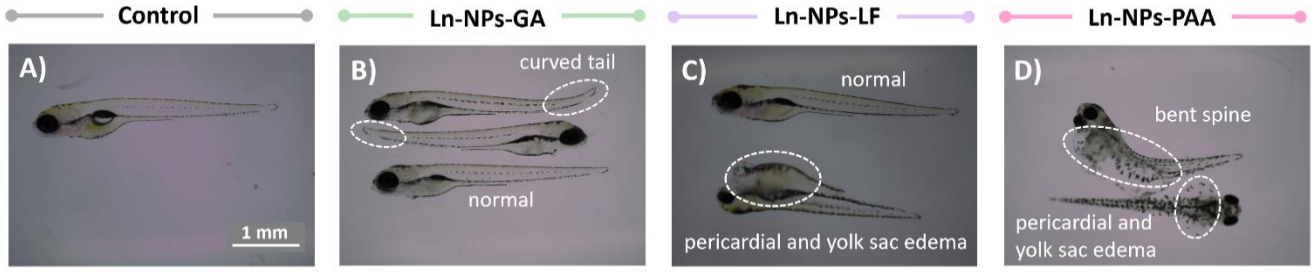

Figure S10. Visual assessment of zebrafish deformity by light microscopy. Images were taken 5 dpf on zebrafish embryos exposed to (A) no Ln-NPs (control), (B) Ln-NPs-GA, (C) Ln-NPs-LF, and (D) Ln-NPs-PAA, respectively. Ln-NP concentration: 0.5 mg/mL. "normal" indicates zebrafish that were exposed to Ln-NPs but did not show any deformities.

8. References

1. N. Liu, N. Gobeil, P. Evers, I. Gessner, E. M. Rodrigues and E. Hemmer, *Dalton Trans.*, 2020, **49**, 16204-16216.
2. H. Zhang, Y. Li, I. A. Ivanov, Y. Qu, Y. Huang and X. Duan, *Angew. Chem. Int. Ed.*, 2010, **49**, 2865-2868.
3. N. Bogdan, F. Vetrone, G. A. Ozin and J. A. Capobianco, *Nano Lett.*, 2011, **11**, 835-840.
4. C. Homann, E. M. Rodrigues, P. Orsini, K. Savard, C.-B. Togola, M.-M. de Denus-Baillargeon, M. Massabki and E. Hemmer, *Opt. Mater. X*, 2024, **21**, 100290.
5. X. Yi, Z. Xu, Y. Liu, X. Guo, M. Ou and X. Xu, *RSC Adv.*, 2017, **7**, 6278-6287.
6. L. E. Mackenzie, J. A. Goode, A. Vakurov, P. P. Nampi, S. Saha, G. Jose and P. A. Millner, *Sci. Rep.*, 2018, **8**, 1106.